AUSTRALIAN ATOMIC ENERGY COMMISSION
RESEARCH ESTABLISHMENT
LUCAS HEIGHTS

FULL-ENERGY-PEAK EFFICIENCIES OF THREE

GAMMA-RAY DETECTORS

by

G.L. HANNA
D.G. WALKER
P.M. BEACH

April 1967

AUSTRALIAN ATOMIC ENERGY COMMISSION

RESEARCH ESTABLISHMENT

LUCAS HEIGHTS

FULL-ENERGY-PEAK EFFICIENCIES OF THREE

GAMMA-RAY DETECTORS

by

G. L. HANNA

D. G. WALKER

P. M. BEACH

ABSTRACT

Two sodium iodide scintillators and a lithium-drifted germanium detector are used in the analysis by gamma-ray spectrometry of gaseous fission products obtained in sweep-capsule fission product release experiments. A description is given of the measurement of full-energy-peak efficiencies of the three detectors for the source geometries used in counting the fission product samples. Experimental efficiencies are compared with calculated efficiencies for one of the sodium iodide detectors. Measurements made of the resolutions obtained with each detector are also noted.

CONTENTS

1. INTRODUCTION

The development of fuel elements for pebble-bed reactors at Lucas Heights has necessitated a study of their fission product retentivity. The method usually employed for this type of work is the sweep-capsule technique in which specimens undergoing irradiation are continuously swept by a flowing gas which entrains escaping volatile products (e.g. krypton and xenon isotopes) and carries them to a point outside the reactor core where they can be sampled and quantitatively determined.

The fission products collected in this way are generally beta-gamma emitters and it is convenient to analyse the mixture using gamma-ray spectrometry.

Sweep-capsule experiments for the H.T.G.C.R. - ABORIGINE programme began in HIFAR in June 1965, and fission product samples have been analysed with a 400-channel gamma-ray spectrometer (Packard model 16). At the date of this report most of the work had been done with a Harshaw 8F8 well-type sodium iodide (NaI) crystal detector (high sensitivity, low resolution) and a Packard M82 solid cylindrical NaI crystal detector (lower sensitivity, higher resolution). Recently a small lithium-drifted germanium detector (subsequently referred to as Ge-Li) became available and is being used almost to the exclusion of the two NaI detectors.

Full-energy-peak efficiency is the ratio of the number of counts within the full-energy peak of the recorded spectrum to the total number of photons of the corresponding energy emitted by the source. Efficiencies were measured for each detector using the same source geometries as in the fission product release experiments. The energy range covered (0.06 to 1.33 MeV) was dictated by the gamma-ray energies encountered in fission product samples but poor resolution prevented calibration of the Harshaw 8F8 detector at energies above 0.84 MeV. The fission products and their predominant gamma-ray energies are listed in Table 1.

2. EXPERIMENTAL PROCEDURE

2.1 Detector Geometry

The Harshaw 8F8 is a well-type detector with an outside diameter of 2 in. and a total height of 2 in. The well in the sodium iodide itself is 1.5 in. deep and 1.125 in. diameter. The aluminium cover and alumina reflector reduce the actual well diameter to 1 in. but increase the depth to 1.83 in. Efficiencies were measured with sources placed centrally on the bottom of the well.

The Packard M82 detector is a right cylindrical crystal measuring 2 in. diameter by 2 in. high. Sources were placed centrally, directly on top of the detector.

The Ge-Li detector (Figure 1) has a measured volume of 3.85 cm^3 and is 0.7 cm thick. It is located on a cold-finger cryostat inside an aluminium vacuum jacket. The top surface of the detector is 2 cm below the upper wall of the vacuum jacket. Sources were placed centrally on top of the vacuum jacket but not necessarily directly above the axis of the germanium crystal.

2.2 Source Geometry

In sweep-capsule experiments, gas samples are collected in two types of bottles (illustrated in Figure 1). One is a 15 ml serum bottle (with rubber seal and metal fastener) and the other a 5 ml bottle with a B/10 conical neck and polyethylene stopper. Full-energy peaks were determined for each container on each detector.

Gaseous calibration sources (which would exactly duplicate the geometry and physical state of the fission product samples) were not available and it was necessary to use sources prepared from solutions of radioisotopes whose radiations lay within the desired energy range. However, the presence of a solvent gave rise to appreciable self-absorption, particularly with low-energy radiation. Total source activities (in terms of the total rate at which photons of a given energy were generated within the liquid source) were therefore corrected for self-absorption (taking no account of the glass container) using a Monte-Carlo calculation written for an IBM 7040 Computer (see Appendix 1). Values of attenuation coefficients of water were taken from Grodstein (1957).

2.3 Calibration Sources and Counting Technique

Calibration sources were prepared from accurately standardised solutions of the radioisotopes listed in Table 2. Sources of similar strength (calibrated to ± 3 per cent. accuracy) were placed in each type of container by adding accurately weighed quantities of the solutions and making up the volume with water to a constant level. To simulate the geometry of gaseous samples this level was as high as possible.

Sources were counted until about 20,000 counts were accumulated in the full-energy peak. Peak intensities were taken as the difference between the total count under the full-energy peak and the count under a background curve constructed by extrapolating under the peak the immediately adjacent regions of the spectrum.

3. RESULTS AND DISCUSSION

3.1 Efficiencies

Full-energy-peak efficiencies were determined for each of the sources listed in Table 2 and are tabulated in Table 3. It was obvious that an efficiency maximum occurred at about 0.1 MeV with the sodium iodide detectors (and possibly the Ge-Li detector). However, lack of data points between 0.06 and 0.122 MeV made the drawing of efficiency-energy graphs (required for interpolation at energies not used in the calibration) very difficult. To overcome this difficulty the following course was taken:

(1)   The measurements published by Nablo and Martin (1961) on the Harshaw 8F8 detector were used to derive full-energy-peak efficiencies for a 15 ml source. These figures were then plotted with those obtained in this work to give efficiency-energy curve for this combination.

(2)   A 5 ml source of Xe-133 (0.081 MeV) derived from fission product samples was counted on each detector and then transferred under water to a 15 ml container and recounted on the three detectors. Thus, it was possible to calibrate all combinations of source, container and detector against the Harshaw 8F8/15 ml combination at this energy.

These calibration points greatly facilitated drawing of the efficiency-energy curves, shown in Figures 3 to 5. Inspection of Figure 3 reveals that the present results for Harshaw 8F8/15 ml combination agree well with those of Nablo and Martin. Efficiencies at 1.17 and 1.33 MeV could not be measured for this detector owing to poor resolution with the Co-60 source. This is demonstrated by the spectra in Figure 6.

It is of some interest to compare experimental efficiencies with calculated values particularly for the Harshaw 8F8 detector used for the bulk of this work. Detailed calculations for common well-type detectors were done by Snyder (1965, 1966), Snyder and Gyorey (1965), and Snyder and Knoll (1966). Similar calculations for a point source were done by Mishra et al. (1966), and are in very good agreement with those of Snyder for equivalent geometry. Although Snyder examined the effects of size and shape of finite-volume sources he did not consider cylindrical sources greater than 1.4 cm high except where the source occupied the total well volume (Snyder 1965). This latter geometry is similar to that for our 15 ml sources, and calculated and experimental efficiencies are compared in Figure 7. (Note that the calculated values have been corrected for absorption in the aluminium and

alumina surrounding the detector and the glass surrounding the source). Agreement between the two sets of figures is reasonably good but not exact. Below 0.14 MeV the calculated efficiencies are low and above this energy become higher than the experimental points. The disagreement arises, in part at least, from the difference between the experimental and assumed geometries.

One concludes from this comparison that calculated efficiencies must be used with caution; in particular care must be taken to ensure that the source geometry used in a calculation is as similar as possible to that used in practice.

3.2 Resolution

Resolution, expressed as full peak-width at half maximum height (FWHM) is shown as a function of energy in Figure 8. The data plotted were determined at considerably different count rates as the same set of sources were used on detectors of differing efficiencies. However, separate tests using varying source strengths on the one detector showed that the peak-broadening due to count-rate effects was less than 0.5 keV for all measurements. This difference was much smaller than that observed between detectors at a given gamma energy.

The most noteworthy feature of Figure 8 is the high resolution of the Ge-Li detector compared with the NaI detectors. The practical implications of the poor resolution of the Harshaw 8F8 detector are perhaps not fully apparent in this figure However, they are well demonstrated in Figure 6 which shows the twin peaks of Co-60 (1.17 and 1.33 MeV) as recorded on each of the three detectors. Obviously the Harshaw 8F8 detector is of little use unless the incident gamma spectrum is very simple.

4. ACKNOWLEDGEMENTS

5. REFERENCES

Grodstein, G. W. (1957). - NBS Circular No. 583.

Mishra, U. C., Brar, S. S., and Gustafson, P. J. (1965). - Int. J. Appl. Rad. Isotopes. 16 (12) : 697.

Nablo, S. V., and Martin, J. C. (1961). - Int. J. Appl. Rad. Isotopes. 10 (1) : 55.

Snyder, B. J. (1965). - Trans. A.N.S. 8 (2) : 341.

Snyder, B. J. (1966). - Nucleonics, to be published.

Snyder, B. J., and Gyorey, G. C. (1965). - Nucleonics 23 (2) : 80.

Snyder, B. J., and Knoll, G. J. (1966). - Nuclear Instruments and Methods. 40 (2) : 261.

APPENDIX.

COMPUTER PROGRAM SABSORB

```
C       MONTE CARLO CALCULATION OF THE SELF-ABSORPTION CORRECTION
C       FOR A HOMOGENEOUS CYLINDRICAL SOURCE PLACED SYMMETRICALLY IN A
C       WELL CRYSTAL.    PROGRAM MAY ALSO BE USED FOR A PLANE CRYSTAL
C       USING DUMMY ENTRIES FOR THE WELL DIMENSIONS.
        DIMENSION FMT(12)
C       READ CRYSTAL AND SOURCE PARAMETERS
        WRITE(6,100)
        PI=3.141593
      1 READ(5,101)(FMT(I),I=1,12)
        WRITE(6,FMT)
        READ(5,102)H,RI,RO
        WRITE(6,103)H,RI,RO
        READ(5,104)HS,RS,DB,ABSN
        WRITE(6,105)HS,RS,DB,ABSN
        READ(5,106) NRAYS
        DT = H-HS-DB
        SABS = 0.
        NCTR = 0
        DO 84 I = 1,NRAYS
C       SELECT POSITION AND DIRECTION PARAMETERS
        RN = RAND(DUM)
        Y = RN*HS+DB
        RN = RAND(DUM)
        CSPHI = 2.*RN-1.
        IF(Y.GT.H.AND.CSPHI.GT.0.) GO TO 84
        RN = RAND(DUM)
        ALP = PI*RN
        RN = RAND(DUM)
        X=RS*SQRT(RN)
        SNPHI = SQRT(1.-CSPHI*CSPHI)
        SNA=SIN(ALP)
        SN2A=SNA*SNA
        ZL=SQRT((RI*RI)-(X*X*SN2A))
        XBAR = X*COS(ALP)
        TNV = -CSPHI/SNPHI
        V=(ZL-XBAR)*TNV
        IF(Y.GT.H) GO TO 80
        IF(Y-V.GT.H) GO TO 84
        VBAR=(ZL-XBAR-DL)*TNV
        IF(Y-VBAR+DT.GT.H)GO TO 76
     65 IF(Y-VBAR-DB.GT.0.)GO TO 77
C       CALCULATE PATH LENGTH
        PATH = ABS((Y-DB)/CSPHI)
        GO TO 78
     76 PATH = ABS((H-DT-Y)/CSPHI)
        GO TO 78
     77 DL=ZL-SQRT((RS*RS)-(X*X*SN2A))
        PATH = ABS((ZL-XBAR-DL)/SNPHI)
     78 NCTR = NCTR+1
        SABS=SABS+EXP(-ABSN*PATH)
        GO TO 84
```

```
80 VBAR=(ZL-XBAR-DL)*TNV
   IF(Y-V.LE.H)GO TO 65
   RL=SQRT((RO*RO)-(X*X*SN2A))
   IF((Y-H)/TNV.LT.RL-XBAR) GO TO 65
84 CONTINUE
   WRITE(6,109) NRAYS
C  CALCULATE EFFICIENCIES
   XRAYS = NRAYS
   XCTR = NCTR
   GEFF = (XCTR/XRAYS)*100.
   FEFF = (SABS/XCTR)*100.
   TEFF = (SABS/XRAYS)*100.
   WRITE(6,107)GEFF,FEFF,TEFF
   WRITE(6,108)
   WRITE(6,110)
   WRITE(6,108)
   GO TO 1
100 FORMAT(1H1)
101 FORMAT(12A6)
102 FORMAT(3F10.5)
103 FORMAT(29H CRYSTAL PARAMETERS. HEIGHT =,F10.5,18H. OUTSIDE RADIUS =,F10.5,17H. INSIDE RADIUS =
   1,F10.5,1H.)
104 FORMAT(4F10.5)
105 FORMAT(28H SOURCE PARAMETERS. HEIGHT =,F10.5,10H. RADIUS =,F10.5,1
   18H. BASE THICKNESS =,F10.5,15H. ABS. COEFF. =,F10.5,1H.)
106 FORMAT(I8)
107 FORMAT(23H GEOMETRIC EFFICIENCY =,F10.3,10H PER CENT./34H EFFICIEN
   1CY FOR RECORDED PHOTONS =,F10.3,10H PER CENT./31H EFFICIENCY FOR T
   2OTAL PHOTONS =,F10.3,10H PER CENT.)
108 FORMAT(1H0)
109 FORMAT(28H0EFFICIENCIES CALCULATED FOR I8,9H PHOTONS.)
110 FORMAT(25X,40H****************************************)
   END
```

TABLE 1

GAMMA-RAY ENERGIES OF THE FISSION PRODUCTS DETECTED

IN SWEEP-CAPSULE EXPERIMENTS

Nuclide	Gamma Energy (MeV)
Xe-133	0.081
Kr-85m	0.15
Kr-88	0.19
Xe-135	0.250
I-131	0.36
Kr-87	0.4
Kr-85	0.52

TABLE 2

RADIOISOTOPES AND SOURCE STRENGTHS USED IN

CALIBRATING GAMMA SPECTROMETER

Isotope	Gamma Energy (MeV)	Source Strength (μCi)	
		15 ml bottle	5 ml bottle
Am-241	0.06	0.0113	0.0112
	0.06	0.98	1.02
Co-57	0.122	} 0.043	} 0.043
	0.136		
U-235	0.143	} 1.20	} 0.846
	0.185		
Cr-51	0.320	0.98	0.98
Cs-137	0.66	0.107	0.089
Mn-54	0.84	0.086	0.094
Co-60	1.17	} 0.048	} 0.049
	1.33		

TABLE 3

FULL-ENERGY-PEAK EFFICIENCIES

Gamma Energy	Harshaw 8F8		Packard M82		Ge-Li	
	15 ml	5 ml	15 ml	5 ml	15 ml	5 ml
0.06	58.80	75.6	10.24	17.0	1.39	1.78
0.081*	(74.0)	(85.8)	(15.2)	(18.45)	(2.08)	(2.45)
0.122	73.1	82.7	15.74	18.7	0.99	1.27
0.136					0.79	1.02
0.143					0.62	0.76
0.186			10.90	15.23	0.44	0.58
0.32	24.06	26.91	6.44	8.40	0.17	0.20
0.66	7.43	7.80	2.40	3.15	0.036	0.047
0.84	4.80	5.22	1.80	2.61	0.026	0.032
1.17	1.74	1.90	0.86	1.13	0.016	0.019
1.33	1.30	1.50	0.80	1.03	0.013	0.016

* Determined from Nablo and Martin (1960). See Section 3.1 this report.
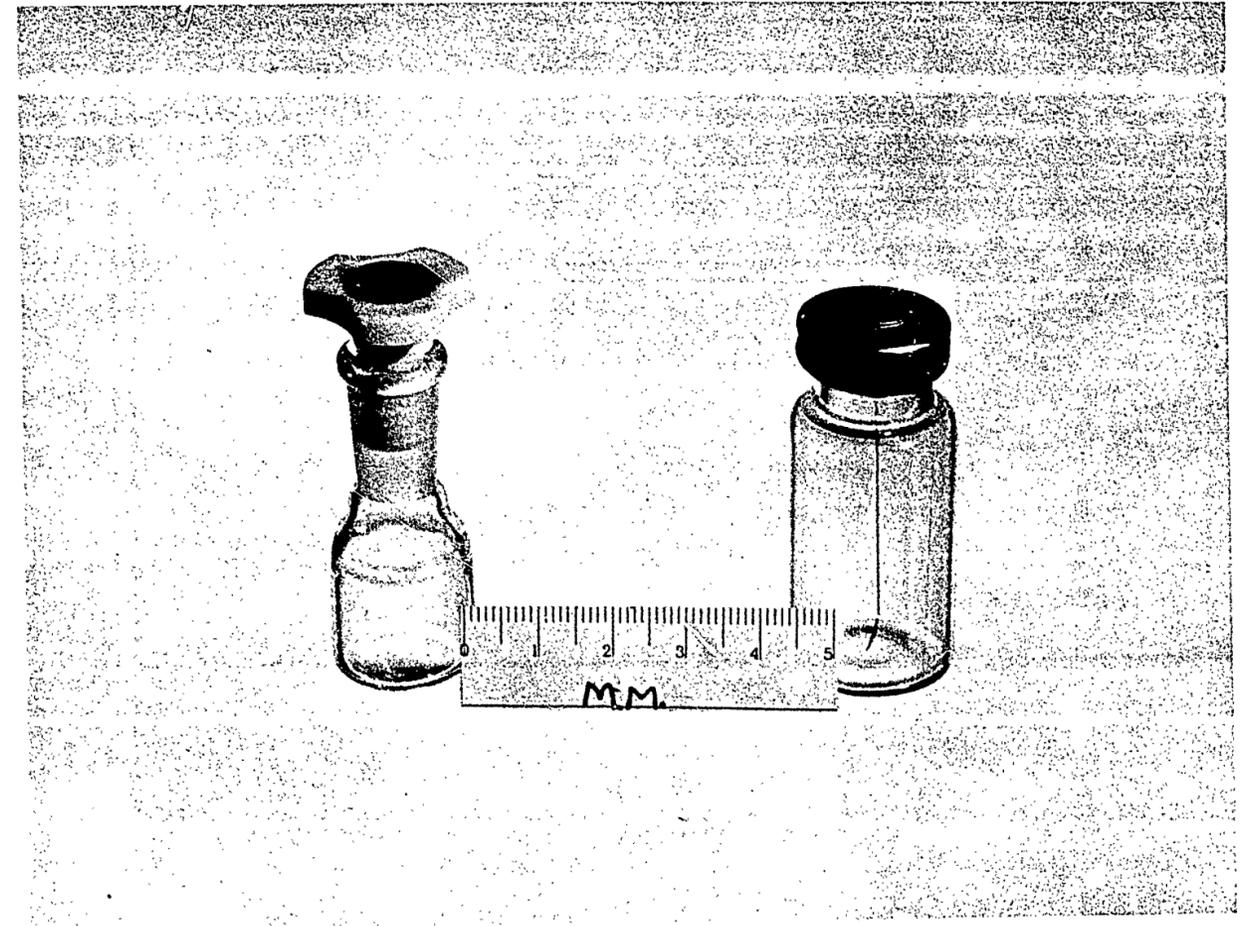
FIGURE 1. FISSION PRODUCT SAMPLING BOTTLES

Ge – Li
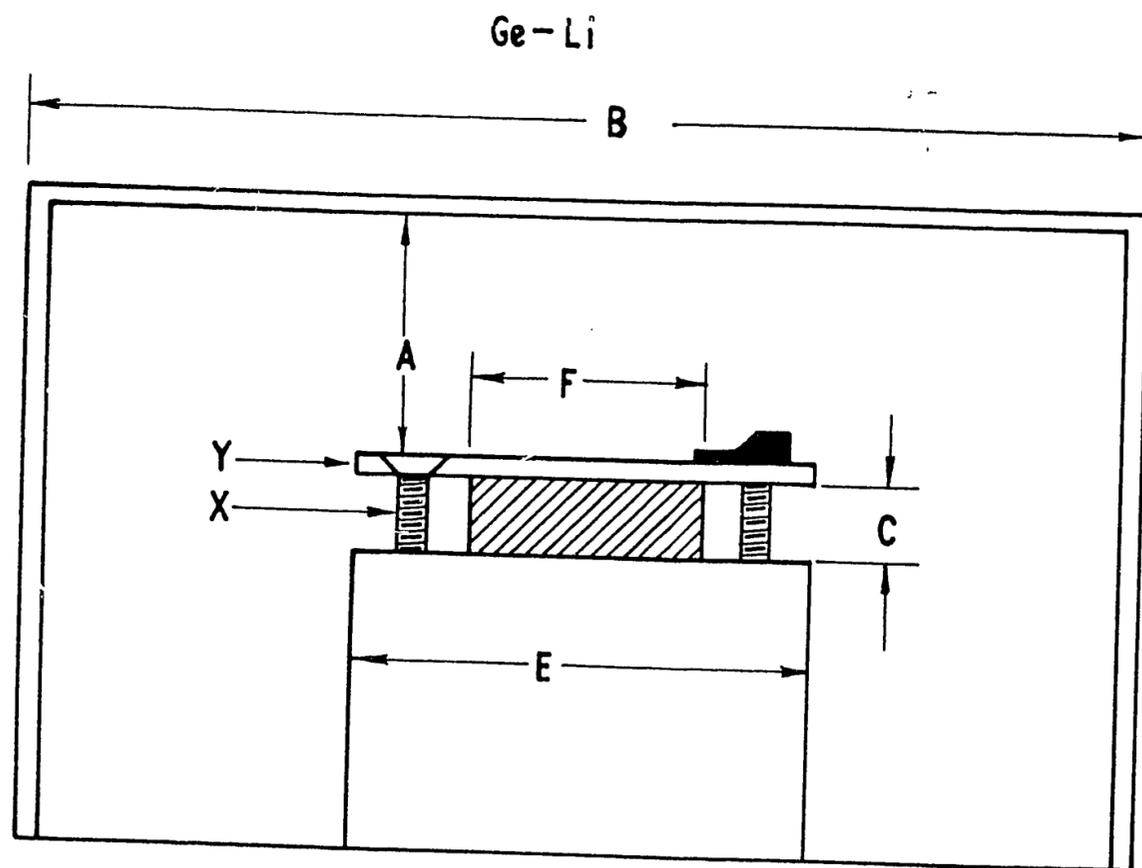
A   =   2·0 cm
B   =   8·9 cm
E   =   4·0 cm
C   =   0·7 cm
F   =   1·9 cm
Y   —   PLASTIC COVER PLATE
X   —   SCREW

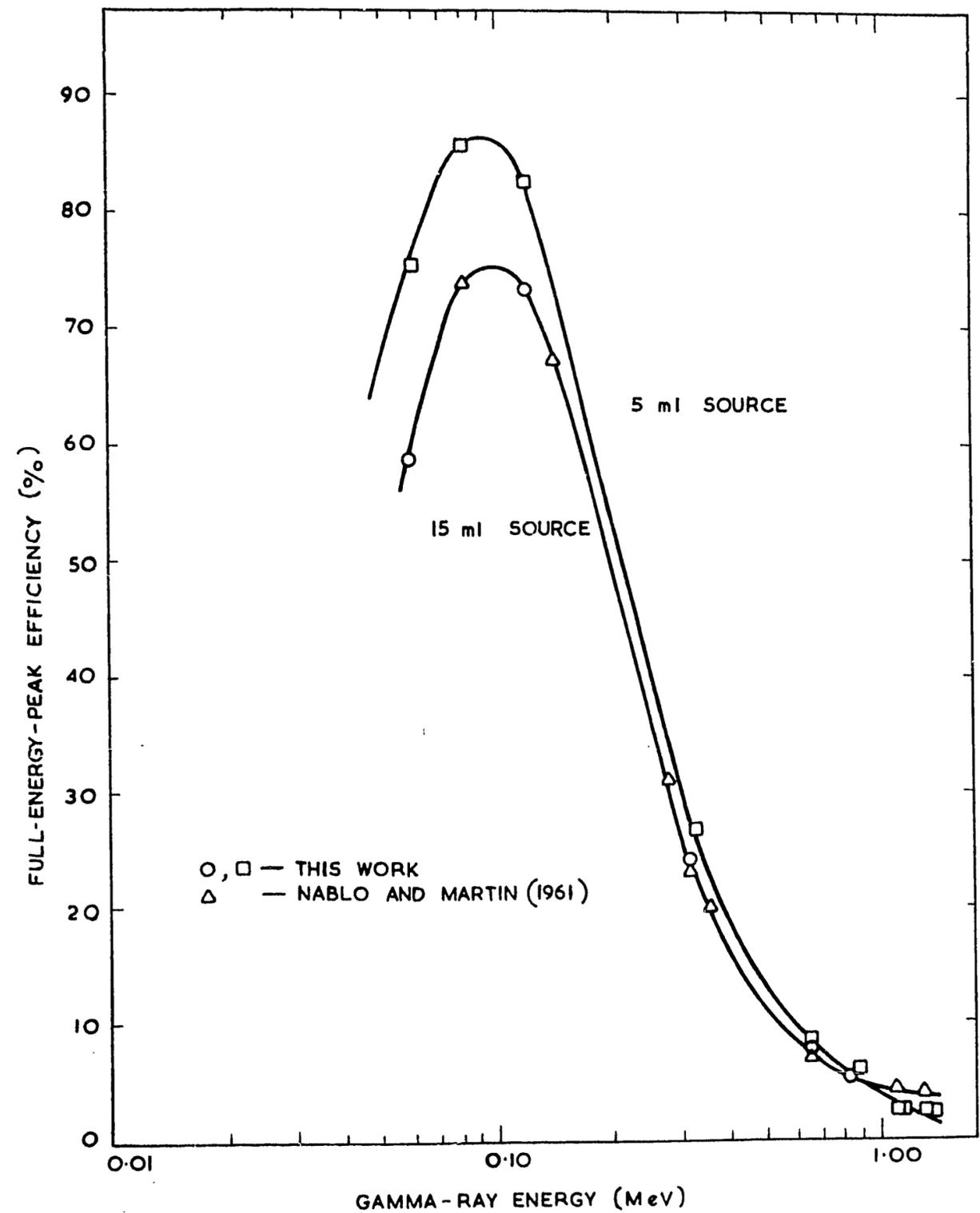FIGURE 2. DIAGRAM OF THE LITHIUM-DRIFTED
GERMANIUM DETECTOR

P1130

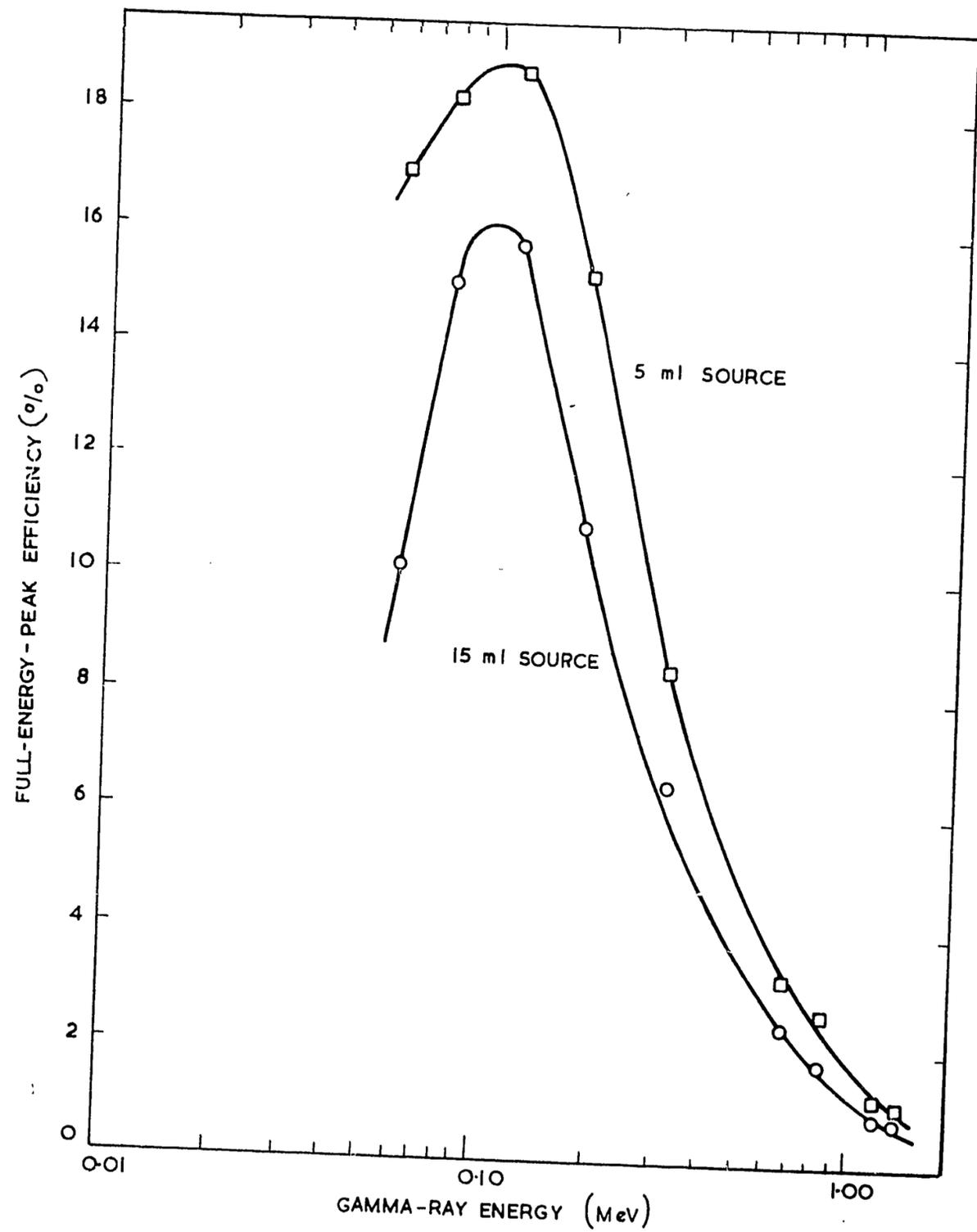FIGURE 3. FULL-ENERGY-PEAK EFFICIENCIES FOR THE
HARSHAW 8F8 DETECTOR

P1130

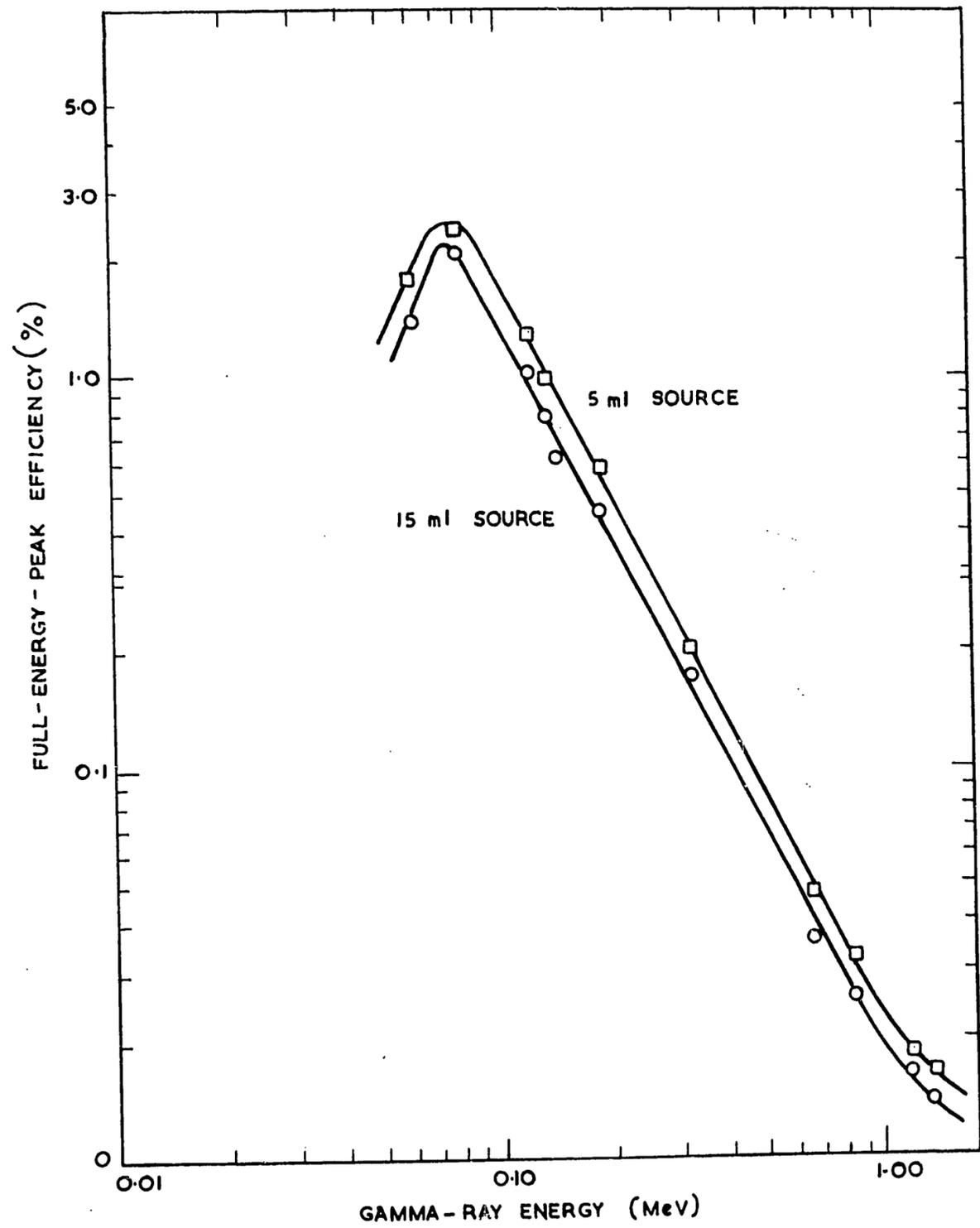FIGURE 4. FULL-ENERGY-PEAK EFFICIENCIES FOR THE
PACKARD M82 DETECTOR

P1130

FIGURE 5. FULL ENERGY-PEAK EFFICIENCIES FOR THE
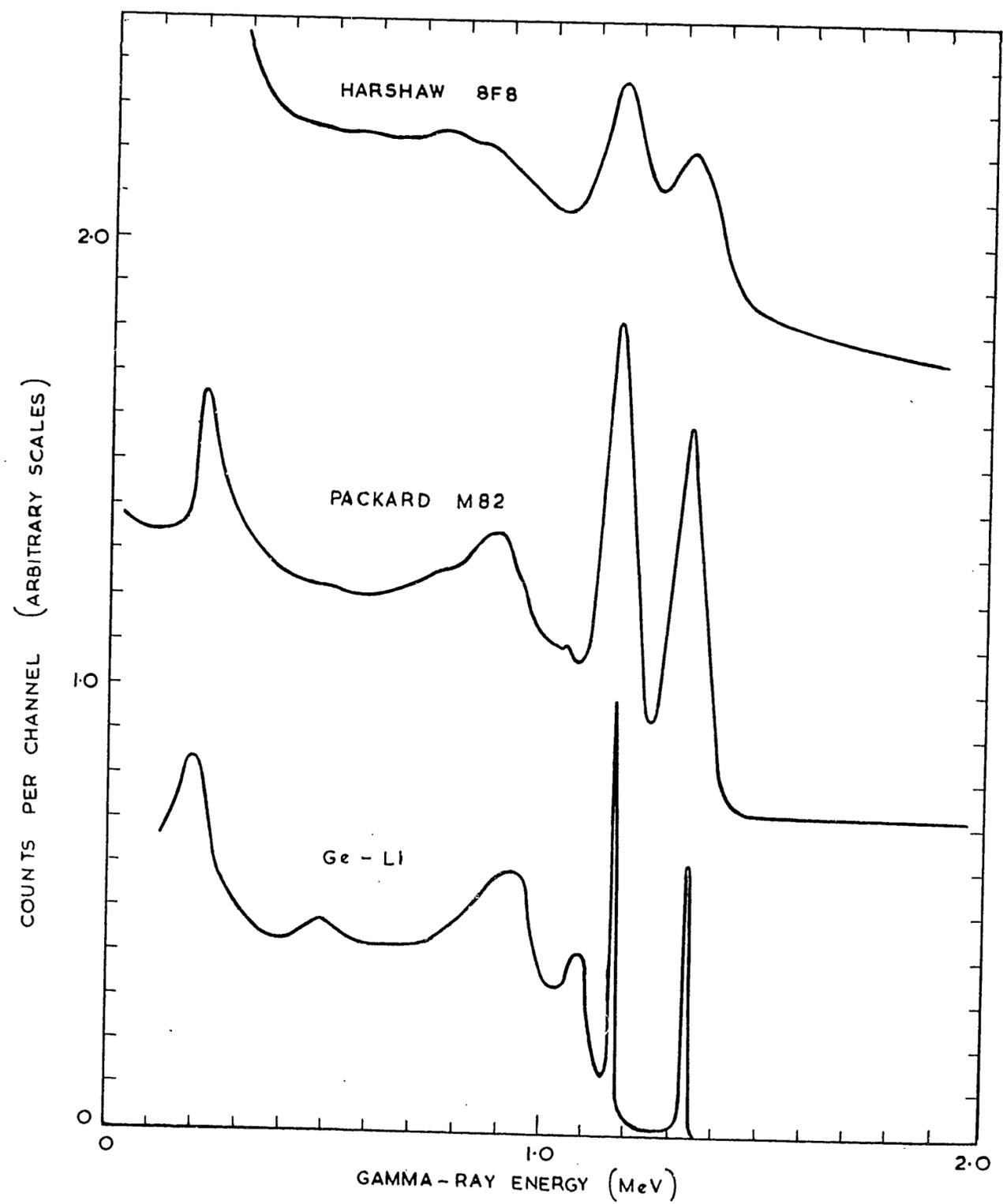Ge-Li DETECTOR

P1130

FIGURE 6. Co-60 SPECTRA RECORDED WITH THE THREE DETECTORS
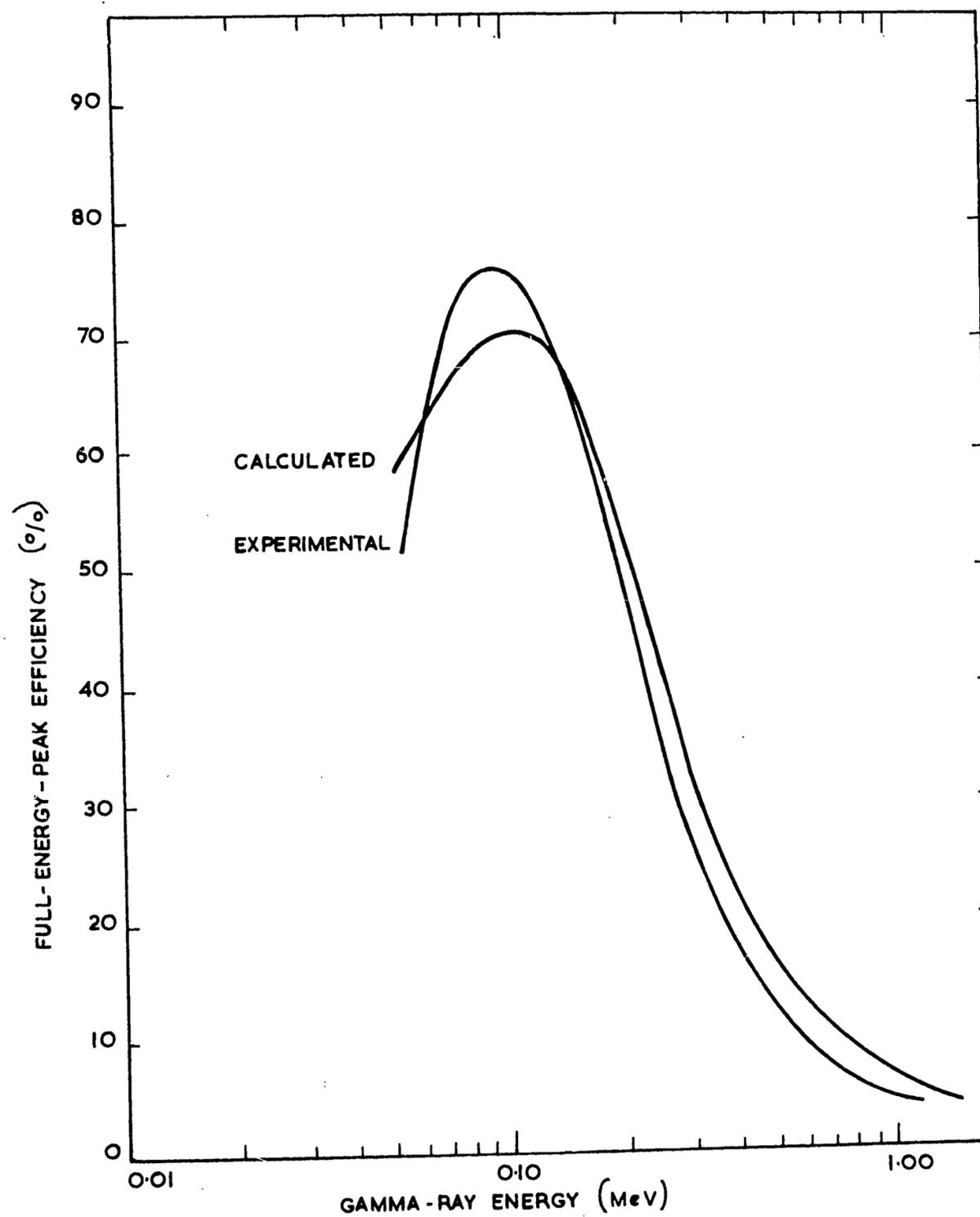

FIGURE 7. EXPERIMENTAL AND CALCULATED EFFICIENCIES FOR A
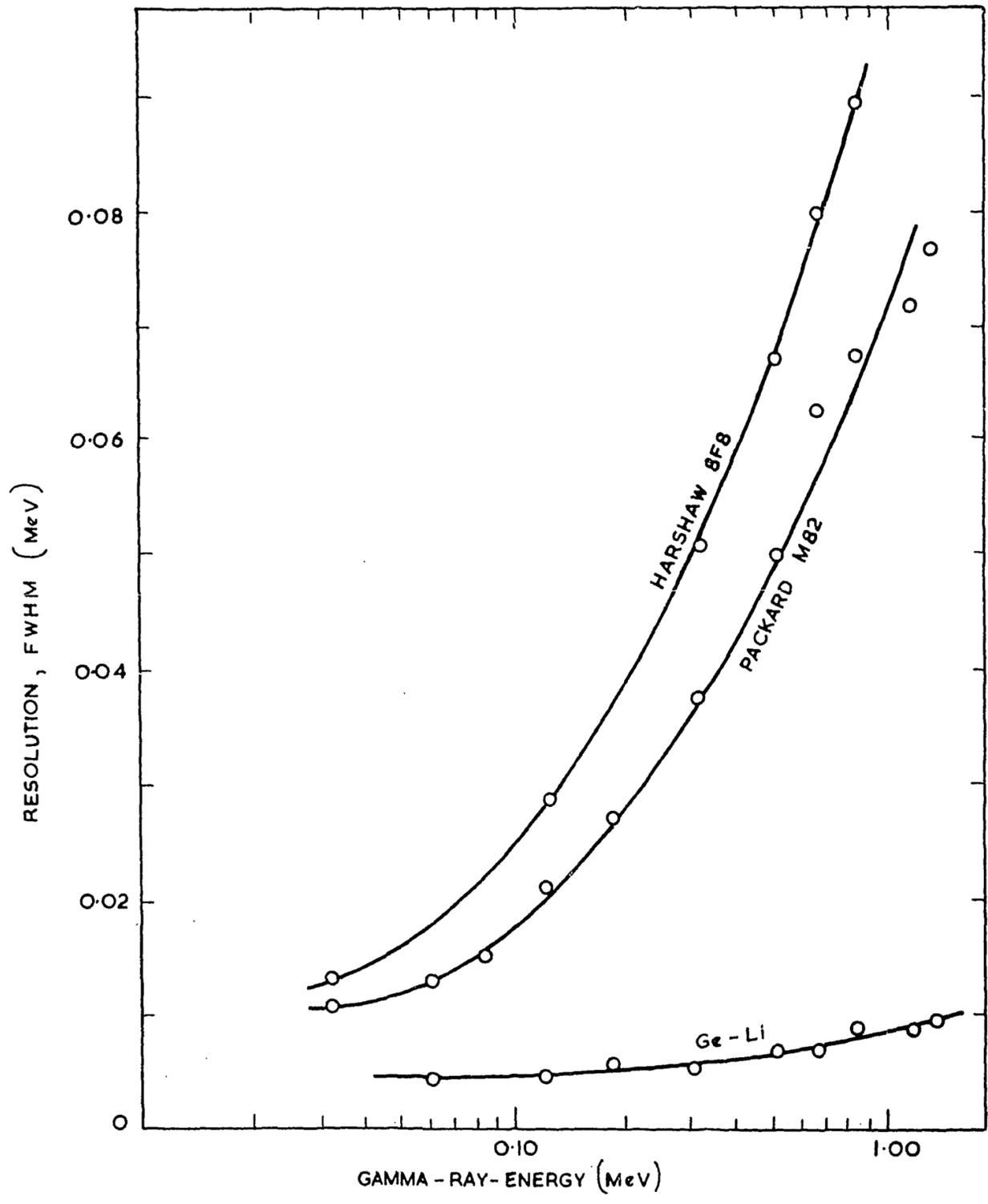15ml SOURCE ON THE HARSHAW 8F8 DETECTOR

P 1130

FIGURE 8. RESOLUTION OF THE THREE DETECTORS AS A
FUNCTION OF GAMMA-RAY ENERGY